

# Exclusive Recognition of CO<sub>2</sub> from Hydrocarbons by Aluminum Formate with Hydrogen-Confined Pore Cavities

Zhaoqiang Zhang,<sup>†</sup> Zeyu Deng,<sup>†</sup> Hayden A. Evans, Dinesh Mullangi, Chengjun Kang, Shing Bo Peh, Yuxiang Wang, Craig M. Brown, John Wang, Pieremanuele Canepa,\* Anthony K. Cheetham,\* and Dan Zhao\*



Cite This: <https://doi.org/10.1021/jacs.3c01705>



Read Online

ACCESS |



Metrics & More

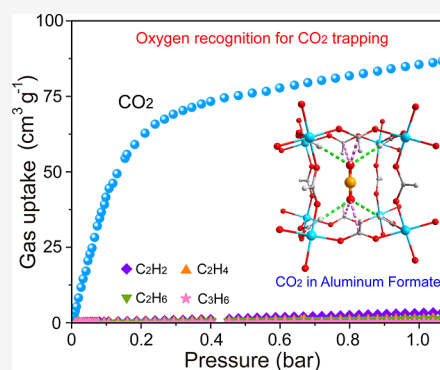


Article Recommendations



Supporting Information

**ABSTRACT:** Exclusive capture of carbon dioxide (CO<sub>2</sub>) from hydrocarbons via adsorptive separation is an important technology in the petrochemical industry, especially for acetylene (C<sub>2</sub>H<sub>2</sub>) production. However, the physicochemical similarities between CO<sub>2</sub> and C<sub>2</sub>H<sub>2</sub> hamper the development of CO<sub>2</sub>-preferential sorbents, and CO<sub>2</sub> is mainly discerned via C recognition with low efficiency. Here, we report that the ultramicroporous material Al(HCOO)<sub>3</sub>, ALF, can exclusively capture CO<sub>2</sub> from hydrocarbon mixtures, including those containing C<sub>2</sub>H<sub>2</sub> and CH<sub>4</sub>. ALF shows a remarkable CO<sub>2</sub> capacity of 86.2 cm<sup>3</sup> g<sup>-1</sup> and record-high CO<sub>2</sub>/C<sub>2</sub>H<sub>2</sub> and CO<sub>2</sub>/CH<sub>4</sub> uptake ratios. The inverse CO<sub>2</sub>/C<sub>2</sub>H<sub>2</sub> separation and exclusive CO<sub>2</sub> capture performance from hydrocarbons are validated via adsorption isotherms and dynamic breakthrough experiments. Notably, the hydrogen-confined pore cavities with appropriate dimensional size provide an ideal pore chemistry to specifically match CO<sub>2</sub> via a hydrogen bonding mechanism, with all hydrocarbons rejected. This molecular recognition mechanism is unveiled by in situ Fourier-transform infrared spectroscopy, X-ray diffraction studies, and molecular simulations.



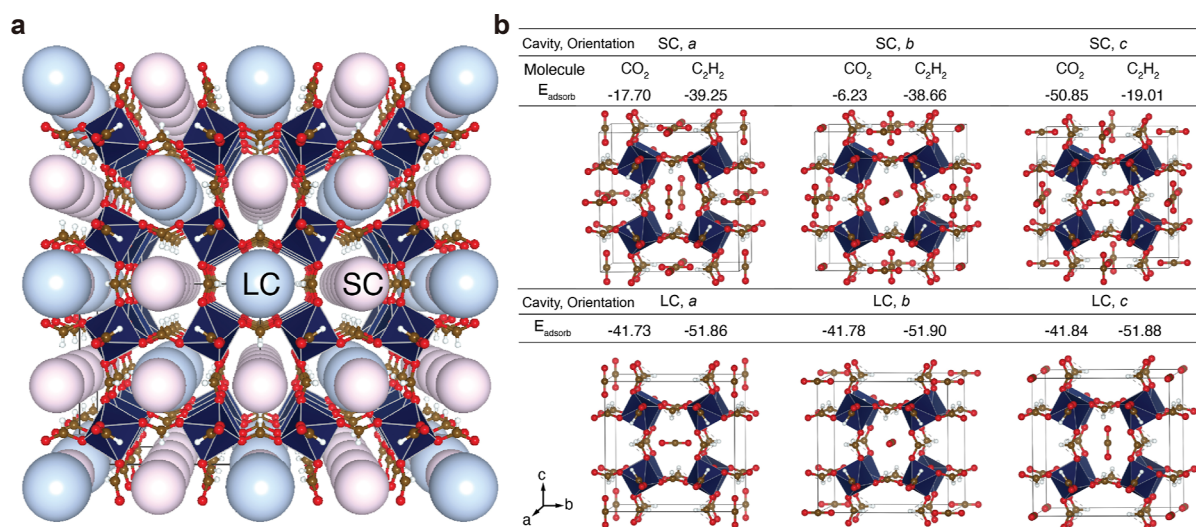
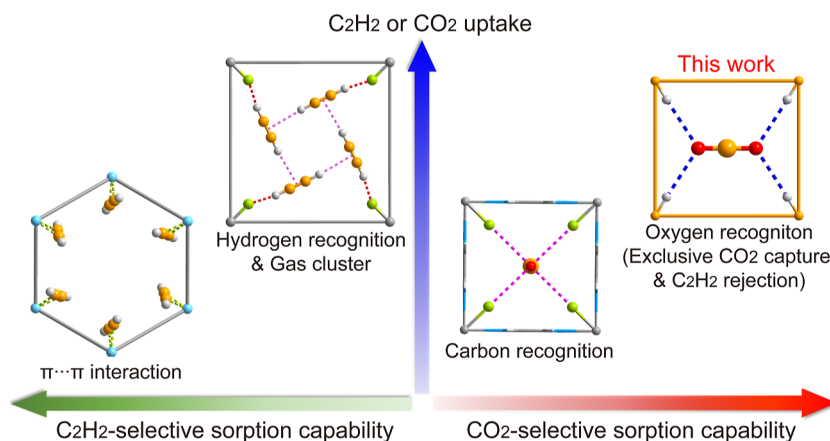
## INTRODUCTION

Selective isolation of CO<sub>2</sub> from hydrocarbons is an essential industrial purification process, given the importance of hydrocarbons as raw materials for the chemical and material industries.<sup>1–4</sup> For example, CO<sub>2</sub> removal is crucial for both natural gas upgrading and the purification of hydrocarbon feedstocks prior to polymerization or chemical derivatization.<sup>4–8</sup> However, conventional techniques predominantly rely on absorption, extraction, and cryogenic distillation, which suffer from drawbacks such as inefficiency, high cost, and energy penalties.<sup>2,3,9</sup> These problems are particularly severe when separating CO<sub>2</sub> from acetylene (C<sub>2</sub>H<sub>2</sub>) as the molecules have almost identical molecular sizes and similar physicochemical properties (Figure S1).<sup>4,10–16</sup> Comparatively, adsorptive separation has shown great promise to supplement the traditional separation methods owing to its improved energy efficiency.<sup>1,17–19</sup> Extensive industrial experience has been accumulated in isolating light (less adsorbed) products. To utilize this experience and account for the presence of CO<sub>2</sub> as an unwanted impurity in typical feed gases (3–50% concentration), CO<sub>2</sub>-selective sorbents are considered to be more advantageous.<sup>4,5,11,14,16,20–25</sup> A major bottleneck in developing sorbents for CO<sub>2</sub> capture from hydrocarbons is to construct the materials with the capability of preferentially trapping CO<sub>2</sub> over C<sub>2</sub>H<sub>2</sub>. A few reports have suggested that the direct production of pure C<sub>2</sub>H<sub>2</sub> via a one-step sorption

procedure using CO<sub>2</sub>-selective sorbents may garner ca. 40% energy saving compared with the process using C<sub>2</sub>H<sub>2</sub>-selective sorbents.<sup>20–23,25–27</sup> Regardless, ubiquitous mechanisms of CO<sub>2</sub> capture, such as those leveraging on the recognition of carbon atoms with acidic chemical functions and/or  $\pi$ -bonds, bind C<sub>2</sub>H<sub>2</sub> similarly to, if not more strongly than, CO<sub>2</sub>, rendering them ineffectual for this separation (Scheme 1).<sup>18</sup> Consequently, exploiting improved operational simplicity and energy efficiency under CO<sub>2</sub>-sequestering process configurations must leverage alternative recognition methods, which are urgently needed.

Ultramicroporous metal–organic frameworks (MOFs, pore size  $\leq 7.0$  Å), self-assembled by linking molecular units with well-defined shapes into periodic frameworks, are a sub-class of hybrid porous materials that distinguish themselves as promising candidates to address challenges of gas separations, especially light hydrocarbon separations.<sup>1,17,28–33</sup> Compared with nanoporous sorbents, the reduced pore dimensions and increased multiplicity of molecularly discriminating host–guest

Received: February 15, 2023

Scheme 1. Proposed Strategies for the Construction of C<sub>2</sub>H<sub>2</sub>- and CO<sub>2</sub>-Selective Porous Materials

**Figure 1.** (a) Schematic illustration of the pore structure of ALF with two kinds of pore cavities, LC (pale blue balls) and SC (light purple balls), with pore windows confined by hydrogen atoms. (b) Computed heats of adsorption ( $E_{\text{adsorb}}$ , kJ/mol per molecule) of CO<sub>2</sub> and C<sub>2</sub>H<sub>2</sub> in ALF with density functional theory: C<sub>2</sub>H<sub>2</sub> and CO<sub>2</sub> adsorbed into LC and SC at three different orientations (CO<sub>2</sub> is used as a guide to show different orientations).

interactions can markedly enhance the gas separation performance. Among them, the inverse CO<sub>2</sub>/C<sub>2</sub>H<sub>2</sub> separation was rarely investigated due to limited knowledge of the relationships between pore chemistry and CO<sub>2</sub> preferential sorption behavior over C<sub>2</sub>H<sub>2</sub>. Recently, inverse CO<sub>2</sub>/C<sub>2</sub>H<sub>2</sub> adsorption was realized via the strategy to target the C atom in CO<sub>2</sub>, but the capacity and selectivity were still moderate. For example, the hybrid ultramicroporous material, SIFSIX-3-Ni, is a prototypical example of inverse-selective material for CO<sub>2</sub>/C<sub>2</sub>H<sub>2</sub> separation.<sup>4</sup> The electronegative F atoms on the pore walls possess high CO<sub>2</sub> affinity via F...C interactions. In contrast, due to the capability of these sites to interact with H atoms of C<sub>2</sub>H<sub>2</sub>, the CO<sub>2</sub>/C<sub>2</sub>H<sub>2</sub> selectivity remained only moderate.<sup>4</sup> Although the related approaches leveraging electron transfer effects have afforded viable pore chemistry for inverse CO<sub>2</sub>/C<sub>2</sub>H<sub>2</sub> separation, they are yet to attain attractive CO<sub>2</sub> selectivity or uptake performance.<sup>21</sup> Furthermore, chemisorptive separation was also revealed to show the potential for selective trapping of CO<sub>2</sub> from C<sub>2</sub>H<sub>2</sub>, but the energy input for the adsorbent regeneration is still higher than that of physical adsorptive separation.<sup>20</sup> Considering the tendency for cross-species interaction (simultaneously inter-

acting with C of CO<sub>2</sub> and H of C<sub>2</sub>H<sub>2</sub>) in CO<sub>2</sub>-selective sorbents targeting the C atom during CO<sub>2</sub>/C<sub>2</sub>H<sub>2</sub> separation, we were motivated to search for alternative mechanisms accessible to ultramicroporous frameworks as a basis for CO<sub>2</sub> capacity and CO<sub>2</sub>/C<sub>2</sub>H<sub>2</sub> selectivity enhancements. We envisaged that incorporating specific electropositive recognition sites for the electronegative O atoms of CO<sub>2</sub> would exert opposite affinity for the acidic H atoms of C<sub>2</sub>H<sub>2</sub> and other hydrocarbons, thus realizing favorable CO<sub>2</sub> capture performance.

Recently, we have shown that the robust ultramicroporous material, aluminum formate (Al(HCOO)<sub>3</sub> or ALF), exhibits a strong affinity for CO<sub>2</sub> capture from dried flue gases containing a mixture of CO<sub>2</sub> and N<sub>2</sub>.<sup>34</sup> ALF, which adopts a ReO<sub>3</sub>-type structure,<sup>35</sup> contains two types of cavities (Figure 1a). Three-quarters of the ALF cavities are smaller cavities (indicated as SC), in which the C–H groups from the bridging formate ligands are perfectly arranged to provide an ideal, hydrogen-bonded docking site for CO<sub>2</sub> (Figures 1a and S2). The hand-in-glove arrangement is so perfect that CO<sub>2</sub> acts as a template for forming the structure of the parent as-made compound, ALF·3/4CO<sub>2</sub>·1/4(HCOOH)·1/4H<sub>2</sub>O.<sup>36</sup> A quarter of the

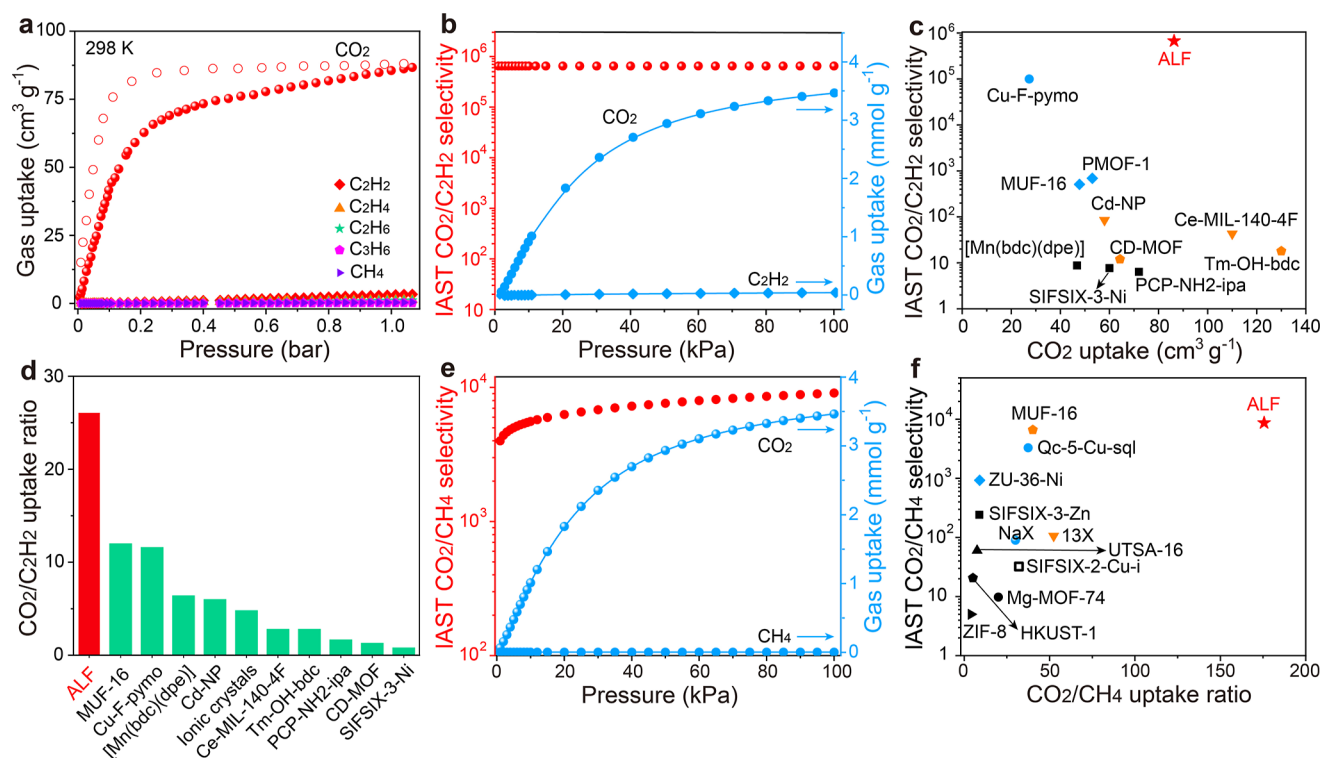


**Figure 2.** (a)  $\text{CO}_2$  and hydrocarbon sorption isotherms on ALF at 298 K. (b) Predicted mixture adsorption isotherms and selectivity of ALF based on IAST for a 50/50  $\text{CO}_2/\text{C}_2\text{H}_2$  mixture at 298 K. (c) Comparison of IAST  $\text{CO}_2/\text{C}_2\text{H}_2$  (50/50) selectivity and  $\text{CO}_2$  uptake for state-of-the-art  $\text{CO}_2$ -selective materials. (d) Comparison of  $\text{CO}_2/\text{C}_2\text{H}_2$  uptake ratios at 298 K and 1 bar between ALF and other  $\text{CO}_2$ -selective materials. (e) Predicted mixture adsorption isotherms and selectivity of ALF based on IAST for a 50/50  $\text{CO}_2/\text{CH}_4$  mixture at 298 K. (f) Comparison of IAST  $\text{CO}_2/\text{CH}_4$  (50/50) selectivity and  $\text{CO}_2/\text{CH}_4$  uptake ratios of selected porous materials at 298 K and 1 bar.

cavities in ALF are larger cavities (LC), and there are no formate C–H groups for such hydrogen bonding, but the pore window is restricted by two H atoms. Thus, both kinds of pore cavities in ALF are confined by H atoms.

In light of the above observations, we explored whether the unique hydrogen-confined pore cavities of ALF would make it a suitable candidate for the separation of  $\text{CO}_2$ -containing hydrocarbon mixtures, especially for  $\text{CO}_2/\text{C}_2\text{H}_2$  and  $\text{CO}_2/\text{CH}_4$  mixtures. We show that ALF achieves an exclusive  $\text{CO}_2$  capture behavior with high capacity from hydrocarbons. Notably, ALF shows the ultrahigh  $\text{CO}_2/\text{C}_2\text{H}_2$  separation selectivity of  $6.5 \times 10^5$ , which sets a new benchmark for inverse  $\text{CO}_2/\text{C}_2\text{H}_2$  separation. We also present data for separating  $\text{CO}_2$  from several  $\text{C}_1$ ,  $\text{C}_2$ , and  $\text{C}_3$  hydrocarbons. The dynamic breakthrough experiments confirmed the performance of ALF for highly efficient  $\text{CO}_2$  capture from hydrocarbons and inverse separation of  $\text{CO}_2/\text{C}_2\text{H}_2$  mixtures. The pore environments investigated by molecular simulations show that the electrostatic potential of the pore surface is complementary to  $\text{CO}_2$ , with  $\text{CO}_2$  captured via  $\text{H}\cdots\text{O}$  and  $\text{C}\cdots\text{O}$  interactions. The ease of ALF synthesis using inexpensive and widely available precursors ( $\text{Al}(\text{OH})_3$  and formic acid) is another advantage that bodes well for future scale-up development.

## RESULTS AND DISCUSSION

**Synthesis and Characterization of Aluminum Formate.** The as-made ALF was synthesized according to a previously reported procedure by the reaction of  $\text{Al}(\text{OH})_3$  and  $\text{Na}_2\text{CO}_3$  in formic acid solution at mild conditions and then activated at vacuum, giving rise to activated ALF.<sup>36</sup> The pore dimensions of two kinds of cavities, SC and LC (Figures 1a

and S3), are very similar to the dimensions of  $\text{CO}_2$  and  $\text{C}_2\text{H}_2$  but smaller than those of other  $\text{C}_2$  and  $\text{C}_3$  hydrocarbons. The purity of the as-synthesized bulk samples was established by comparing the experimentally collected and simulated powder X-ray diffraction (PXRD) patterns (Figure S4). Additionally, ALF can retain its crystallinity after being exposed to air for one month.<sup>34</sup> The thermal stability of the activated material was further evaluated by thermogravimetric analysis (TGA), and the result shows that ALF is stable up to 503 K (230 °C) (Figure S5).

**$\text{CO}_2$  and Hydrocarbon Sorption Performance.** The small pore sizes of all cavities make ALF an interesting candidate for  $\text{CO}_2$  adsorption and separation. Single-component  $\text{CO}_2$  and  $\text{C}_2\text{H}_2$  gas sorption isotherms on ALF were first collected at 298 K. It is intriguing to find that ALF adsorbs  $\text{CO}_2$  with high capacity but shows negligible  $\text{C}_2\text{H}_2$  uptakes (Figure 2a). To further investigate the behavior of ALF, we collected the sorption isotherms of other hydrocarbons, including  $\text{CH}_4$ ,  $\text{C}_2\text{H}_4$ ,  $\text{C}_2\text{H}_6$ , and  $\text{C}_3\text{H}_6$ . The results show that all these larger molecules are excluded by ALF. The combination of the exclusive  $\text{CO}_2$  capture performance with high capacity and selectivity against these important hydrocarbons in ALF appears remarkable, with rare precedents.<sup>5</sup> Detailed analysis indicates that the capacity of  $\text{CO}_2$  can reach  $86.2 \text{ cm}^3 \text{ g}^{-1}$  ( $3.85 \text{ mmol g}^{-1}$ ) at 1 bar and 298 K, but  $\text{C}_2\text{H}_2$  uptake is only  $3.3 \text{ cm}^3 \text{ g}^{-1}$  under the same conditions. Even over a broad temperature range, ALF still exhibits high  $\text{CO}_2$  uptakes (273–323 K, Figure S6) and negligible or low  $\text{C}_2\text{H}_2$  uptakes (253–333 K, Figure S7). Notably, the  $\text{CO}_2$  uptake is much higher than that of most state-of-the-art materials used for inverse  $\text{CO}_2/\text{C}_2\text{H}_2$  separation (Table S1), such as MUF-16



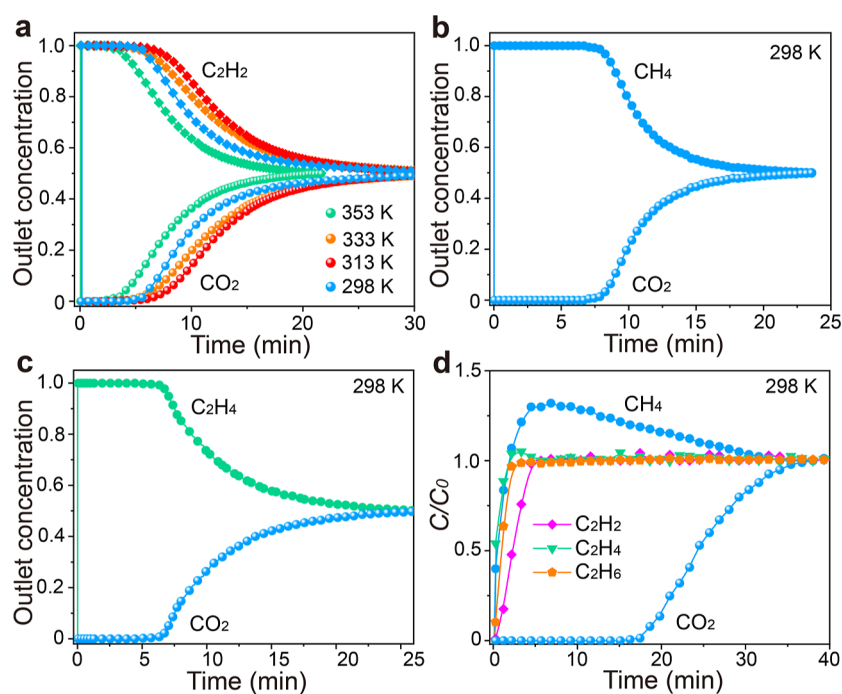


**Figure 3.** (a–c) Experimental fixed-bed breakthrough results for equimolar  $\text{CO}_2/\text{C}_2\text{H}_2$  (a),  $\text{CO}_2/\text{CH}_4$  (b), and  $\text{CO}_2/\text{C}_2\text{H}_4$  (c) mixtures. (d) Breakthrough curves of the  $\text{CO}_2/\text{C}_2\text{H}_2/\text{C}_2\text{H}_4/\text{C}_2\text{H}_6/\text{CH}_4$  (1/1/1/1/1) mixture on ALF at 298 K. Note: a flow rate of  $2.0 \text{ mL min}^{-1}$  was used for all breakthrough experiments.

( $47.8 \text{ cm}^3 \text{ g}^{-1}$ ),<sup>5</sup> Cd-NP ( $58 \text{ cm}^3 \text{ g}^{-1}$ ),<sup>27</sup> SIFSIX-3-Ni ( $60.5 \text{ cm}^3 \text{ g}^{-1}$ ),<sup>4</sup> and even the inverse sieving material Cu-F-pymo ( $26.7 \text{ cm}^3 \text{ g}^{-1}$ ).<sup>11</sup>

To quantitatively evaluate the separation potential of ALF, the ideal adsorbed solution theory (IAST) was utilized to estimate the separation selectivity toward an equimolar  $\text{CO}_2/\text{C}_2\text{H}_2$  mixture (Figure 2b). The inverse selectivity can reach  $6.5 \times 10^5$ , far exceeding those of most MOFs with inverse  $\text{CO}_2/\text{C}_2\text{H}_2$  separation capabilities (Figure 2c and Table S1). For example, the inverse selectivities of Cd-NP<sup>11</sup> and MUF-16<sup>5</sup> are  $10^5$  and 510, respectively. According to the IAST calculations, ALF features a high  $\text{CO}_2$  uptake of  $\sim 3.5 \text{ mmol g}^{-1}$  from an equimolar  $\text{CO}_2/\text{C}_2\text{H}_2$  mixture while exhibiting a negligible  $\text{C}_2\text{H}_2$  uptake (Figure 2b). The uptake ratio is another important parameter demonstrating the preference and separation potential of the adsorbent for certain molecules over others. For ALF, the calculated  $\text{CO}_2/\text{C}_2\text{H}_2$  uptake ratio is 26.1, much higher than that reported for benchmark materials, such as Cu-F-pymo (11.6),<sup>11</sup> MUF-16 (12),<sup>5</sup> Ce-MIL-140-4F (2.8),<sup>21</sup> and Tm-OH-bdc (2.8)<sup>22</sup> (Figure 2d). Such a high  $\text{CO}_2$  capacity and  $\text{CO}_2/\text{C}_2\text{H}_2$  uptake ratio signify that ALF sets a new benchmark for inverse  $\text{CO}_2/\text{C}_2\text{H}_2$  adsorption and separation (Figure 2c). Additionally, the uptake ratios and separation selectivity of ALF for other hydrocarbons are equally impressive (Figures 2e,f and S8, Table S2). The equimolar  $\text{CO}_2/\text{CH}_4$  separation selectivity and  $\text{CO}_2/\text{CH}_4$  uptake ratio can reach  $\sim 9100$  and  $\sim 172$ , respectively, higher than those on MUF-16 (6686 and 40, respectively).<sup>5</sup> These results underline the outstanding separation performance of ALF in removing  $\text{CO}_2$  from hydrocarbons.

**$\text{CO}_2$  Separation Performance from Hydrocarbons.** To intuitively evaluate the performance of  $\text{CO}_2$  dynamic trapping and inverse sieving effects for  $\text{CO}_2/\text{C}_2\text{H}_2$ , fixed-bed breakthrough experiments were carried out (Figure 3). As expected, a complete separation of  $\text{CO}_2/\text{C}_2\text{H}_2$  was observed with high-

purity  $\text{C}_2\text{H}_2$  immediately harvested from an ALF-packed column (Figure 3a). The calculated  $\text{CO}_2$  trapped amount on ALF from the breakthrough experiment was  $\sim 2.32 \text{ mmol g}^{-1}$ , with the  $\text{C}_2\text{H}_2$  productivity of  $\sim 5.4 \text{ mmol g}^{-1}$ —32 times higher than that on Cu-F-pymo ( $0.166 \text{ mmol g}^{-1}$ ).<sup>11</sup> The dynamic uptake of  $\text{CO}_2$  in these runs was similar to our observations for static sorption experiments (Figure 2a). The  $\text{CO}_2$  capture capacity was  $\sim 2.75 \text{ mmol g}^{-1}$  at 313 K, higher than those at other temperatures (2.64 and  $2.0 \text{ mmol g}^{-1}$  at 323 and 353 K, respectively). The  $\text{CO}_2$  breakthrough time also follows the order that it is longer at 313 K compared with those at other temperatures. To further validate the temperature effect on the  $\text{CO}_2$  capture performance, single-component  $\text{CO}_2$  breakthrough curves were collected (Figure S9). Similarly, the results show that there is a suitable temperature favorable for  $\text{CO}_2$  mass transfer. At 313 K, the dynamic  $\text{CO}_2$  sorption amount is  $\sim 3.1 \text{ mmol g}^{-1}$ . Additionally, the higher flow rates and the existence of humidity would not compromise the  $\text{CO}_2$  capture and  $\text{C}_2\text{H}_2$  production performances of ALF (Figure S10). The  $\text{CO}_2$  capture performance of ALF is meritorious and sets a new benchmark for inverse  $\text{CO}_2/\text{C}_2\text{H}_2$  separations with the inverse sieving effect for  $\text{C}_2\text{H}_2$ . Furthermore, benefiting from the sieving effect for hydrocarbons, ALF is an exclusive and promising material to efficiently trap  $\text{CO}_2$  from  $\text{CO}_2$ -containing hydrocarbon mixtures (Figure 3b–d). In particular, ALF, with its low cost and easy synthesis procedure, is a very promising porous material to remove  $\text{CO}_2$  in natural gas sweetening, biogas processing, and hydrocarbon upgrading, especially  $\text{C}_2\text{H}_2$  purification.

**$\text{CO}_2$  Trapping Mechanism.** It is reasonable that ALF with small pore sizes exhibits excellent size-selective sieving behavior toward mixtures of  $\text{CO}_2$  with other large gas molecules, such as  $\text{CH}_4$ ,  $\text{C}_2\text{H}_4$ ,  $\text{C}_2\text{H}_6$ , and  $\text{C}_3\text{H}_6$ . However, the inverse sieving effect for  $\text{CO}_2$  and  $\text{C}_2\text{H}_2$  (where the kinetic

diameters of both molecules are 3.3 Å) is unexpected. To understand the origins of this puzzling behavior, we investigated the in situ FTIR spectrum of CO<sub>2</sub>-loaded ALF (Figure S11). The C=O bond peak of ~1600 cm<sup>-1</sup> (antisymmetric stretching vibration) is blue-shifted to ~1615 cm<sup>-1</sup>, and the bending vibration peaks of C–H bond at ~467 and ~490 cm<sup>-1</sup> are blue-shifted to ~474 and ~500 cm<sup>-1</sup>, respectively. These changes indicate that the trapped CO<sub>2</sub> molecules in ALF interact with the H or C atoms of formate groups in the pore channels. The new emerging peak at ~1405 cm<sup>-1</sup> is linked to the symmetric formate mode due to subtle structural modifications from CO<sub>2</sub> adsorption. Furthermore, the electrostatic potential of CO<sub>2</sub> can complement the pore surface potential surrounded by H and C atoms (Figures S12–S14). Notably, ALF can exclusively trap CO<sub>2</sub> from hydrocarbons owing to the combination of the specific electro-positive pore windows and cavities restricted by H and C atoms with suitable pore chemistry and the narrow ultramicro pore. The mutual repulsion effect between H atoms of formate and H atoms of C<sub>2</sub>H<sub>2</sub> leads to a repulsive interaction that hinders adsorption and also lowers the heat of adsorption (see below). This simplified electrostatic picture can qualitatively explain why only CO<sub>2</sub> can be trapped, with C<sub>2</sub>H<sub>2</sub> being excluded. In situ C<sub>2</sub>H<sub>2</sub> synchrotron diffraction experiments on ALF further confirmed that no C<sub>2</sub>H<sub>2</sub> entered ALF over the course of 30 min time scales at 253 and 313 K (Figure S15 and Table S4, S5). This aligns with the presented isotherm data and verifies that ALF is selective against C<sub>2</sub>H<sub>2</sub>.

We performed dispersion-corrected density functional theory (DFT-D3) calculations to compare the heats of adsorption ( $E_{\text{adsorb}}$ ) of CO<sub>2</sub> and C<sub>2</sub>H<sub>2</sub> in ALF (Figure 1b). Although C<sub>2</sub>H<sub>2</sub> does not readily adsorb into ALF, the results show that  $E_{\text{adsorb}}$  of C<sub>2</sub>H<sub>2</sub> into SC and LC of ALF are favorable and broadly similar (around 39 and 52 kJ/mol for C<sub>2</sub>H<sub>2</sub> in its preferred orientations in SC and LC, respectively) to those of CO<sub>2</sub> (around 51 and 42 kJ/mol for CO<sub>2</sub> in its preferred orientations in SC and LC, respectively). However, since all the C–H bonds of the formate ligands point toward SC instead of LC, C<sub>2</sub>H<sub>2</sub> shows a preference for LC, whereas CO<sub>2</sub> prefers SC. By inspecting the results of adsorption calculations, we observed that CO<sub>2</sub> and C<sub>2</sub>H<sub>2</sub> manifest preferred orientations in SC. CO<sub>2</sub> aligns toward the C–H bonds, whereas C<sub>2</sub>H<sub>2</sub> favors the perpendicular directions (Figure 1b). In this way, the CO<sub>2</sub> molecules establish stabilizing hydrogen bonds with the C–H groups, which is not possible in the case of C<sub>2</sub>H<sub>2</sub>. In LC, CO<sub>2</sub> and C<sub>2</sub>H<sub>2</sub> do not have preferred orientations in terms of adsorption energy, suggesting that they can show positional disorder. Based on these results, we believe that the separation of CO<sub>2</sub>/C<sub>2</sub>H<sub>2</sub> is not driven by thermodynamic effects since the heats of adsorption are both favorable. It appears to be a kinetic effect, which is consistent with the observation of modest C<sub>2</sub>H<sub>2</sub> uptake into ALF at 313 K (Figure S7).

To address this kinetic effect, we evaluated the translation barriers of both CO<sub>2</sub> and C<sub>2</sub>H<sub>2</sub> to verify whether the adsorption of these molecules in ALF may be kinetically hindered. Nudged elastic band calculations were performed, and the energy barriers of translating C<sub>2</sub>H<sub>2</sub> and CO<sub>2</sub> within ALF in the dilute limit (one molecule per unit cell of ALF) were computed (Tables S6, S7 and Figure S16). There are two main types of translation mechanisms that can happen in the ALF structure: (1) translation of a guest molecule (CO<sub>2</sub> or C<sub>2</sub>H<sub>2</sub>) between two small cavities and (2) guest molecule

translation between a small and a large cavity. For scenario (1) (and from symmetry considerations on the ALF structure), both C<sub>2</sub>H<sub>2</sub> and CO<sub>2</sub> should rotate by 90° when exchanging between two neighboring small cavities. For example, a CO<sub>2</sub> departing from its most stable adsorbing configuration (along the *c* direction in SC) will initially align along the crystallographic direction when exchanged with a nearby small cavity. This step will be followed by a rotation of CO<sub>2</sub> to reach its most stable orientation along the *c* direction. As for scenario (2), the translation can only happen between molecules aligned in the *b* direction, where the molecule points toward a large cavity and any direction in the nearby large cavity. We also found that both CO<sub>2</sub> and C<sub>2</sub>H<sub>2</sub> can only translate along C=O or C–H bond directions, respectively, through the aperture between two cavities without rotations. The energy barriers of translating CO<sub>2</sub> between two adjacent small cavities are ~654 or ~292 meV, depending on the direction of translation (Figure S16), whereas for C<sub>2</sub>H<sub>2</sub>, the barriers are nearly direction-independent (~437 and ~535 meV). As for the translation between a small and a large cavity, CO<sub>2</sub> shows barriers of ~152 or ~624 meV. In contrast, the same translation mechanism for C<sub>2</sub>H<sub>2</sub> is accompanied by unsurmountable translation barriers of ~821 or ~1018 meV. These results show that C<sub>2</sub>H<sub>2</sub> access to the large cavity is highly impeded and that the passage of CO<sub>2</sub> between both types of apertures (between cavities) is easier than that of C<sub>2</sub>H<sub>2</sub>. Although the large cavity in ALF provides a higher heat of adsorption for C<sub>2</sub>H<sub>2</sub>, it remains inaccessible due to the extremely high activation barriers.

## CONCLUSIONS

Efficient CO<sub>2</sub> capture from hydrocarbons is required to achieve both carbon neutrality and sustainable development and is also important for producing high-purity hydrocarbons. We report that ALF shows excellent exclusive CO<sub>2</sub> separation performance from CO<sub>2</sub>-containing hydrocarbon mixtures. Notably, the hydrogen-confined pore cavity with an electropositive surface and appropriate dimension provides a perfect pore chemistry to devotedly match the potential of CO<sub>2</sub> via weak H···O and C···O interactions. The exclusive CO<sub>2</sub> trapping behavior was validated via single-component gas adsorption and dynamic breakthrough experiments using CO<sub>2</sub>-containing hydrocarbon mixtures. ALF exhibits a benchmark inverse sieving separation performance for CO<sub>2</sub>/C<sub>2</sub>H<sub>2</sub> mixtures. High-purity C<sub>2</sub>H<sub>2</sub> (99.99%) with a productivity of 5.4 mmol g<sup>-1</sup> was obtained via only a one-step sorption procedure. Equally, the performance of ALF for separating CO<sub>2</sub> from methane is also impressive, suggesting that it could find utility in biogas processing.<sup>37</sup> The exclusive CO<sub>2</sub> capture behavior in an ultramicroporous material with hydrogen-confined pore cavities provides deep insights into the bottom-up design strategies of advanced porous materials used for molecular recognition.

## ASSOCIATED CONTENT

### Supporting Information

The Supporting Information is available free of charge at <https://pubs.acs.org/doi/10.1021/jacs.3c01705>.

Details of experimental section, material synthesis, gas adsorption and separation procedures, FTIR spectra, PXRD patterns, TGA, and DFT calculations (PDF)

## AUTHOR INFORMATION

## Corresponding Authors

**Pieremanuele Canepa** – Department of Chemical and Biomolecular Engineering, National University of Singapore, Singapore 117585, Singapore; Department of Materials Science and Engineering, National University of Singapore, Singapore 117575, Singapore; [orcid.org/0000-0002-5168-9253](https://orcid.org/0000-0002-5168-9253); Email: [pcanepa@nus.edu.sg](mailto:pcanepa@nus.edu.sg)

**Anthony K. Cheetham** – Department of Materials Science and Engineering, National University of Singapore, Singapore 117575, Singapore; Materials Research Laboratory, University of California, Santa Barbara, California 93106, United States; [orcid.org/0000-0003-1518-4845](https://orcid.org/0000-0003-1518-4845); Email: [akc30@cam.ac.uk](mailto:akc30@cam.ac.uk)

**Dan Zhao** – Department of Chemical and Biomolecular Engineering, National University of Singapore, Singapore 117585, Singapore; [orcid.org/0000-0002-4427-2150](https://orcid.org/0000-0002-4427-2150); Email: [chezhao@nus.edu.sg](mailto:chezhao@nus.edu.sg)

## Authors

**Zhaoqiang Zhang** – Department of Chemical and Biomolecular Engineering, National University of Singapore, Singapore 117585, Singapore; [orcid.org/0000-0002-9172-2871](https://orcid.org/0000-0002-9172-2871)

**Zeyu Deng** – Department of Materials Science and Engineering, National University of Singapore, Singapore 117575, Singapore; [orcid.org/0000-0003-0109-9367](https://orcid.org/0000-0003-0109-9367)

**Hayden A. Evans** – Center for Neutron Research, National Institute of Standards and Technology, Gaithersburg, Maryland 20878, United States; [orcid.org/0000-0002-1331-4274](https://orcid.org/0000-0002-1331-4274)

**Dinesh Mullangi** – Department of Materials Science and Engineering, National University of Singapore, Singapore 117575, Singapore; [orcid.org/0000-0003-4012-0587](https://orcid.org/0000-0003-4012-0587)

**Chengjun Kang** – Department of Chemical and Biomolecular Engineering, National University of Singapore, Singapore 117585, Singapore; [orcid.org/0000-0003-0208-2954](https://orcid.org/0000-0003-0208-2954)

**Shing Bo Peh** – Department of Chemical and Biomolecular Engineering, National University of Singapore, Singapore 117585, Singapore; [orcid.org/0000-0002-2250-757X](https://orcid.org/0000-0002-2250-757X)

**Yuxiang Wang** – Department of Chemical and Biomolecular Engineering, National University of Singapore, Singapore 117585, Singapore; [orcid.org/0000-0002-6945-6431](https://orcid.org/0000-0002-6945-6431)

**Craig M. Brown** – Center for Neutron Research, National Institute of Standards and Technology, Gaithersburg, Maryland 20878, United States; [orcid.org/0000-0002-9637-9355](https://orcid.org/0000-0002-9637-9355)

**John Wang** – Department of Materials Science and Engineering, National University of Singapore, Singapore 117575, Singapore; [orcid.org/0000-0001-6059-8962](https://orcid.org/0000-0001-6059-8962)

Complete contact information is available at:

<https://pubs.acs.org/10.1021/jacs.3c01705>

## Author Contributions

<sup>†</sup>Z.Z. and Z.D. authors contributed equally.

## Notes

The authors declare the following competing financial interest(s): A patent has been filed by the National University of Singapore based on the present results (SG Patent Application No. 10202260362V).

## ACKNOWLEDGMENTS

This work was supported by the Ministry of Education—Singapore (MOE2019-T2-1-093, MOE-T2EP10122-0002, MOE-000381-01), the Energy Market Authority of Singapore (EMA-EP009-SEGC-020), the Agency for Science, Technology, and Research (U2102d2004, U2102d2012), and the National Research Foundation Singapore (NRF-CRP26-2021RS-0002). Certain commercial equipment, instruments, or materials are identified in this document. This identification does not imply recommendation or endorsement by the National Institute of Standards and Technology, nor does it imply that the products identified are necessarily the best available for the purpose.

## REFERENCES

- (1) Adil, K.; Belmabkhout, Y.; Pillai, R. S.; Cadiau, A.; Bhatt, P. M.; Assen, A. H.; Maurin, G.; Eddaoudi, M. Gas/vapour separation using ultra-microporous metal-organic frameworks: Insights into the structure/separation relationship. *Chem. Soc. Rev.* **2017**, *46*, 3402–3430.
- (2) Zhou, D.; Zhang, X.; Mo, Z.; Xu, Y.; Tian, X.; Li, Y.; Chen, X.; Zhang, J. Adsorptive separation of carbon dioxide: From conventional porous materials to metal-organic frameworks. *EnergyChem* **2019**, *1*, 100016.
- (3) Hu, Z.; Wang, Y.; Shah, B.; Zhao, D. CO<sub>2</sub> capture in metal-organic framework adsorbents: An engineering perspective. *Adv. Sustainable Syst.* **2019**, *3*, 1800080.
- (4) Chen, K. J.; Scott, H. S.; Madden, D. G.; Pham, T.; Kumar, A.; Bajpai, A.; Lusi, M.; Forrest, K. A.; Space, B.; Perry, J. J.; Zaworotko, M. J. Benchmark C<sub>2</sub>H<sub>2</sub>/CO<sub>2</sub> and CO<sub>2</sub>/C<sub>2</sub>H<sub>2</sub> separation by two closely related hybrid ultramicroporous materials. *Chem* **2016**, *1*, 753–765.
- (5) Qazvini, O. T.; Babarao, R.; Telfer, S. G. Selective capture of carbon dioxide from hydrocarbons using a metal-organic framework. *Nat. Commun.* **2021**, *12*, 197.
- (6) Cui, W. G.; Hu, T. L.; Bu, X. H. Metal-organic framework materials for the separation and purification of light hydrocarbons. *Adv. Mater.* **2020**, *32*, No. e1806445.
- (7) Siegelman, R. L.; Kim, E. J.; Long, J. R. Porous materials for carbon dioxide separations. *Nat. Mater.* **2021**, *20*, 1060–1072.
- (8) Kim, E. J.; Siegelman, R. L.; Jiang, H.; Forse, A. C.; Lee, J.; Martell, J. D.; Milner, P. J.; Falkowski, J. M.; Neaton, J. B.; Reimer, J. A.; Weston, S. C.; Long, J. R. Cooperative carbon capture and steam regeneration with tetraamine-appended metal-organic frameworks. *Science* **2020**, *369*, 392–396.
- (9) Li, J. R.; Sculley, J.; Zhou, H. C. Metal-organic frameworks for separations. *Chem. Rev.* **2012**, *112*, 869–932.
- (10) Gong, W.; Cui, H.; Xie, Y.; Li, Y.; Tang, X.; Liu, Y.; Cui, Y.; Chen, B. Efficient C<sub>2</sub>H<sub>2</sub>/CO<sub>2</sub> separation in ultramicroporous metal-organic frameworks with record C<sub>2</sub>H<sub>2</sub> storage density. *J. Am. Chem. Soc.* **2021**, *143*, 14869–14876.
- (11) Shi, Y.; Xie, Y.; Cui, H.; Ye, Y.; Wu, H.; Zhou, W.; Arman, H.; Lin, R. B.; Chen, B. Highly selective adsorption of carbon Dioxide over acetylene in an ultramicroporous metal-organic framework. *Adv. Mater.* **2021**, *33*, 2105880.
- (12) Ye, Y.; Ma, Z.; Lin, R. B.; Krishna, R.; Zhou, W.; Lin, Q.; Zhang, Z.; Xiang, S.; Chen, B. Pore space partition within a metal-organic framework for highly efficient C<sub>2</sub>H<sub>2</sub>/CO<sub>2</sub> separation. *J. Am. Chem. Soc.* **2019**, *141*, 4130–4136.
- (13) Zhang, J.; Chen, X. Optimized acetylene/carbon dioxide sorption in a dynamic porous crystal. *J. Am. Chem. Soc.* **2009**, *131*, 5516–5521.
- (14) Eguchi, R.; Uchida, S.; Mizuno, N. Inverse and high CO<sub>2</sub>/C<sub>2</sub>H<sub>2</sub> sorption selectivity in Flexible organic-inorganic ionic crystals. *Angew. Chem., Int. Ed.* **2012**, *51*, 1635.
- (15) Gao, J.; Qian, X.; Lin, R. B.; Krishna, R.; Wu, H.; Zhou, W.; Chen, B. Mixed metal-organic framework with multiple binding sites



for efficient C<sub>2</sub>H<sub>2</sub>/CO<sub>2</sub> separation. *Angew. Chem., Int. Ed.* **2020**, *59*, 4396–4400.

(16) Gu, Y.; Zheng, J. J.; Otake, K. I.; Shivanna, M.; Sakaki, S.; Yoshino, H.; Ohba, M.; Kawaguchi, S.; Wang, Y.; Li, F.; Kitagawa, S. Host-guest interaction modulation in porous coordination polymers for inverse selective CO<sub>2</sub>/C<sub>2</sub>H<sub>2</sub> Separation. *Angew. Chem., Int. Ed.* **2021**, *60*, 11688.

(17) Lin, R. B.; Zhang, Z.; Chen, B. Achieving high performance metal-organic framework materials through pore engineering. *Acc. Chem. Res.* **2021**, *54*, 3362–3376.

(18) Zhang, Z.; Kang, C.; Peh, S.; Shi, D.; Yang, F.; Liu, Q.; Zhao, D. Efficient adsorption of acetylene over CO<sub>2</sub> in bioinspired covalent organic frameworks. *J. Am. Chem. Soc.* **2022**, *144*, 14992–14996.

(19) Wang, S.; Lee, J.; Wahiduzzaman, M.; Park, J.; Muschi, M.; Martineau-Corcoss, C.; Tissot, A.; Cho, K.; Marrot, J.; Shepard, W.; Maurin, G.; Chang, J.; Serre, C. A robust large-pore zirconium carboxylate metal-organic framework for energy-efficient water-sorption-driven refrigeration. *Nat. Energy* **2018**, *3*, 985–993.

(20) Choi, D.; Kim, D.; Kang, D.; Kang, M.; Chae, Y.; Hong, C. Highly selective CO<sub>2</sub> separation from a CO<sub>2</sub>/C<sub>2</sub>H<sub>2</sub> mixture using a diamine-appended metal-organic framework. *J. Mater. Chem. A* **2021**, *9*, 21424–21428.

(21) Zhang, Z.; Peh, S. B.; Krishna, R.; Kang, C.; Chai, K.; Wang, Y.; Shi, D.; Zhao, D. Optimal pore chemistry in an ultramicroporous metal-organic framework for benchmark inverse CO<sub>2</sub>/C<sub>2</sub>H<sub>2</sub> separation. *Angew. Chem., Int. Ed.* **2021**, *60*, 17198–17204.

(22) Ma, D.; Li, Z.; Zhu, J.; Zhou, Y.; Chen, L.; Mai, X.; Liufu, M.; Wu, Y.; Li, Y. Inverse and highly selective separation of CO<sub>2</sub>/C<sub>2</sub>H<sub>2</sub> on a thulium-organic framework. *J. Mater. Chem. A* **2020**, *8*, 11933–11937.

(23) Li, L.; Wang, J.; Zhang, Z.; Yang, Q.; Yang, Y.; Su, B.; Bao, Z.; Ren, Q. Inverse adsorption separation of CO<sub>2</sub>/C<sub>2</sub>H<sub>2</sub> mixture in cyclodextrin-based metal-organic frameworks. *ACS Appl. Mater. Interfaces* **2019**, *11*, 2543–2550.

(24) Foo, M. L.; Matsuda, R.; Hijikata, Y.; Krishna, R.; Sato, H.; Horike, S.; Hori, A.; Duan, J.; Sato, Y.; Kubota, Y.; Takata, M.; Kitagawa, S. An adsorbate discriminatory gate effect in a flexible porous coordination polymer for selective adsorption of CO<sub>2</sub> over C<sub>2</sub>H<sub>2</sub>. *J. Am. Chem. Soc.* **2016**, *138*, 3022–3030.

(25) Cai, L. Z.; Yao, Z. Z.; Lin, S. J.; Wang, M. S.; Guo, G. C. Photoinduced electron-transfer (PIET) strategy for selective adsorption of CO<sub>2</sub> over C<sub>2</sub>H<sub>2</sub> in a MOF. *Angew. Chem., Int. Ed.* **2021**, *60*, 18223–18230.

(26) Cui, J.; Qiu, Z.; Yang, L.; Zhang, Z.; Cui, X.; Xing, H. Kinetic-sieving of carbon dioxide from acetylene through a novel sulfonic ultramicroporous material. *Angew. Chem., Int. Ed.* **2022**, *61*, No. e202208756.

(27) Xie, Y.; Cui, H.; Wu, H.; Lin, R. B.; Zhou, W.; Chen, B. Electrostatically driven selective adsorption of carbon dioxide over acetylene in an ultramicroporous material. *Angew. Chem., Int. Ed.* **2021**, *60*, 9604–9609.

(28) Lin, R. B.; Li, L.; Zhou, H. L.; Wu, H.; He, C.; Li, S.; Krishna, R.; Li, J.; Zhou, W.; Chen, B. Molecular sieving of ethylene from ethane using a rigid metal-organic framework. *Nat. Mater.* **2018**, *17*, 1128–1133.

(29) Ding, Q.; Zhang, Z.; Yu, C.; Zhang, P.; Wang, J.; Cui, X.; He, C.; Deng, S.; Xing, H. Exploiting equilibrium-kinetic synergetic effect for separation of ethylene and ethane in a microporous metal-Organic framework. *Sci. Adv.* **2020**, *6*, No. eaaz4322.

(30) Islamoglu, T.; Chen, Z.; Wasson, M. C.; Buru, C. T.; Kirlikovali, K. O.; Afrin, U.; Mian, M. R.; Farha, O. K. Metal-organic frameworks against toxic chemicals. *Chem. Rev.* **2020**, *120*, 8130–8160.

(31) Ji, Z.; Wang, H.; Canossa, S.; Wuttke, S.; Yaghi, O. M. Pore chemistry of metal-organic frameworks. *Adv. Funct. Mater.* **2020**, *30*, 2000238.

(32) Wang, H.; Liu, Y.; Li, J. Designer metal-organic frameworks for size-exclusion-based hydrocarbon separations: progress and challenges. *Adv. Mater.* **2020**, *32*, No. e2002603.

(33) Zhang, Z. Q.; Peh, S. B.; Kang, C.; Chai, K.; Zhao, D. Metal-organic frameworks for C<sub>6</sub>–C<sub>8</sub> hydrocarbon separations. *EnergyChem* **2021**, *3*, 100057.

(34) Evans, A.; Mullangi, D.; Deng, Z.; Wang, Y.; Peh, S. B.; Wei, F.; Wang, J.; Brown, C. M.; Zhao, D.; Canepa, P.; Cheetham, A. K.; Canepa, P.; Cheetham, K. A. Aluminum formate, Al(HCOO)<sub>3</sub>: An earth-abundant, scalable, and highly selective material for CO<sub>2</sub> capture. *Sci. Adv.* **2022**, *8*, No. eade1473.

(35) Evans, H. A.; Wu, Y.; Seshadri, R.; Cheetham, A. K. Perovskite-related ReO<sub>3</sub>-type structures. *Nat. Rev. Mater.* **2020**, *5*, 196–213.

(36) Tian, Y.; Zhao, Y.; Xu, H.; Chi, C. CO<sub>2</sub> Template Synthesis of Metal Formates with a ReO<sub>3</sub> Net. *Inorg. Chem.* **2007**, *46*, 1612–1616.

(37) Ryckebosch, E.; Drouillon, M.; Vervaeren, H. Techniques for transformation of biogas to biomethane. *Biomass Bioenergy* **2011**, *35*, 1633–1645.